Optical frequency standard with Sr^+: A theoretical many-body approach

Chiranjib Sur , K. V. P. Latha, Rajat K. Chaudhuri, B. P. Das
NAPP Theory Group, Indian Institute of Astrophysics, Bangalore 560 034, India
D. Mukherjee
Indian Association for the Cultivation of Science, Kolkata - 700 032, India

February 2, 2008

Abstract

Demands from several areas of science and technology have lead to a worldwide search for accurate optical clocks with an uncertainty of 1 part in 10^{18}, which is 10^3 times more accurate than the present day cesium atomic clocks based on microwave frequency regime. In this article we discuss the electric quadrupole and the hyperfine shifts in the $5s\,^2S_{1/2} \longrightarrow 4d\,^2D_{5/2}$ clock transition in Sr^+, one of the most promising candidates for next generation optical clocks. We have applied relativistic coupled cluster theory for determining the electric quadrupole moment of the $4d\,^2D_{5/2}$ state of $^{88}Sr^+$ and the magnetic dipole (A) and electric quadrupole (B) hyperfine constants for the $5s\,^2S_{1/2}$ and $4d\,^2D_{5/2}$ states which are important in the study of frequency standards with Sr^+. The effects of electron correlation which are very crucial for the accurate determination of these quantities have been discussed.

PACS number(s). : 31.15.Ar, 31.15.Dv, 32.30.Jc, 31.25.Jf, 32.10.Fn

1 Introduction

The frequencies at which atoms emit or absorb electro-magnetic radiation during a transition can be used for defining the basic unit of time [1, 2, 3]. The transitions that are extremely stable, accurately measurable and reproducible can serve as excellent frequency standards [1, 2]. The current frequency standard is based on the ground state hyperfine transition in ^{133}Cs which is in the microwave regime and has an uncertainty of one part in 10^{15} [4]. However, there is a search for even more accurate clocks in the optical regime. The uncertainty of these clocks is expected to be about 1 part in 10^{17} or 10^{18} [5]. Some of the prominent candidates that belong to this category are $^{88}Sr^+$ [6, 7], $^{199}Hg^+$ [8], $^{171}Yb^+$ [9], $^{43}Ca^+$ [10], $^{138}Ba^+$ etc. Indeed detailed studies on these ions will have to be carried out in order to determine their suitability for optical frequency standards. In a recent article [11] Gill and Margolis have discussed the merits of choosing $^{88}Sr^+$ as a candidate for an optical clock. Till recently, the most accurate measurement of an optical frequency was for the clock transition in $^{88}Sr^+$ which has an uncertainty of 3.4 parts in 10^{15} [12]. However, recently, Oskay et al. [13] have measured the optical frequency of $^{199}Hg^+$ to an accuracy of 1.5 parts in 10^{15} and further improvements are expected [14].

In this article we concentrate on strontium ion (Sr^+) which is considered to be one of the leading candidates for an ultra high precision optical clock [11]. The clock transition in this case is $5s\,^2S_{1/2} \longrightarrow 4d\,^2D_{5/2}$ and is observed by using the quantum jump technique in single trapped strontium ion. When an atom interacts with an external field, the standard frequency may be shifted from the resonant frequency. The quality of the frequency standard depends upon the accurate and precise measurement of this shift. To minimize or maintain any shift of the clock frequency, the interaction of the atom with it's surroundings must be controlled. Hence, it is important to have a good knowledge of these shifts so as to minimize them while setting up the frequency standard. Some of these shifts are the linear Zeeman shift, quadratic Zeeman shift, second-order Stark shift, hyperfine shift and electric quadrupole shift. The largest source of uncertainty in frequency shift arises from the electric quadrupole shift of the clock transition because of the interaction of atomic electric quadrupole moment with the gradient of external electric field. In this article we have applied relativistic coupled-cluster (RCC) theory, one of the most accurate atomic many-body theories to calculate the electric quadrupole moment (EQM) and the hyperfine constants for the energy levels involved in the clock transition.

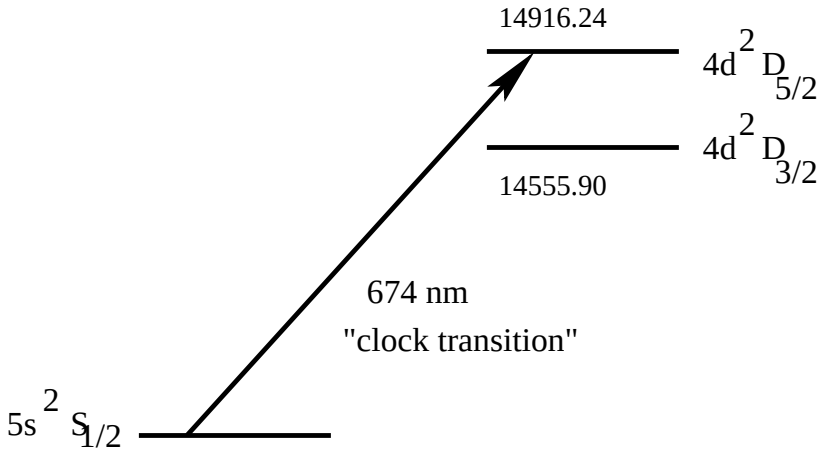

Figure 1: Clock transition in $^{88}Sr^{+}$. Excitation energies of the $4d\ ^2D_{3/2}$and $4d\ ^2D_{5/2}$levels are given in cm^{-1}.

2 Relativistic coupled-cluster theory

The relativistic and dynamical electron correlation effects can be incorporated in many-electron systems through a variety of many-body methods [15, 16, 17, 18]. The relativistic coupled cluster (RCC) method has emerged as one of the most powerful and effective tools for high precision description of electron correlations in many-electron systems [17, 18]. The RCC is an all-order non-perturbative scheme, and therefore, the higher order electron correlation effects can be incorporated more efficiently than using the order-by-order diagrammatic many-body perturbation theory (MBPT). RCC is equivalent to all order relativistic MBPT (RMBPT). The RCC results can therefore be improved by adding the important omitted diagrams with the aid of low order RMBPT. We have applied RCC theory to calculate atomic properties for several systems and more details can be obtained from Ref. [19].

Here we present a brief outline of RCC theory. We begin with N-electron Dirac-Coulomb Hamiltonian (H) which is expressed as

$$H = \sum_{i=1}^{N} \left[c\vec{\alpha_i} \cdot \vec{p_i} + \beta mc^2 + V_N(r_i) \right] + \sum_{i<j}^{N} \frac{e^2}{r_{ij}}\,, \tag{1}$$

with the Fermi vacuum described by the four component Dirac-Fock (DF) state $|\Phi\rangle$. The normal ordered form of the above Hamiltonian is given by

$$H_N = H - \langle\Phi|H|\Phi\rangle = \sum_{ij} \langle i|f|j\rangle \left\{ a_i^\dagger a_j \right\} + \frac{1}{4} \sum_{i,j,k,l} \langle ij||kl\rangle \left\{ a_i^\dagger a_j^\dagger a_l a_k \right\}, \tag{2}$$

where

$$\langle ij||kl\rangle = \langle ij|\frac{1}{r_{12}}|kl\rangle - \langle ij|\frac{1}{r_{12}}|lk\rangle. \tag{3}$$

Following Lindgren's formulation of open-shell CC [20], we express the valence universal wave operator Ω as

$$\Omega = \{\exp(\sigma)\}, \tag{4}$$

and σ being the excitation operator and curly brackets denote the normal ordering. The wave operator Ω acting on the DF reference state gives the exact correlated state. The operator σ has two parts, one corresponding to the core and the other to the valence sector denoted by T and S respectively. In the singles and double (SD) excitation approximation the excitation operator for the core sector is given by

$$T = T_1 + T_2 = \sum_{ap} \left\{ a_p^\dagger a_a \right\} t_a^p + \frac{1}{4} \sum_{abpq} \left\{ a_p^\dagger a_q^\dagger a_b a_a \right\} t_{ab}^{pq}\,, \tag{5}$$

t_a^p and t_{ab}^{pq} being the amplitudes corresponding to single and double excitations respectively. For a single valence system like Sr^+, the excitation operator for the valence sector turns out to be $\exp(S) = \{1 + S\}$ and

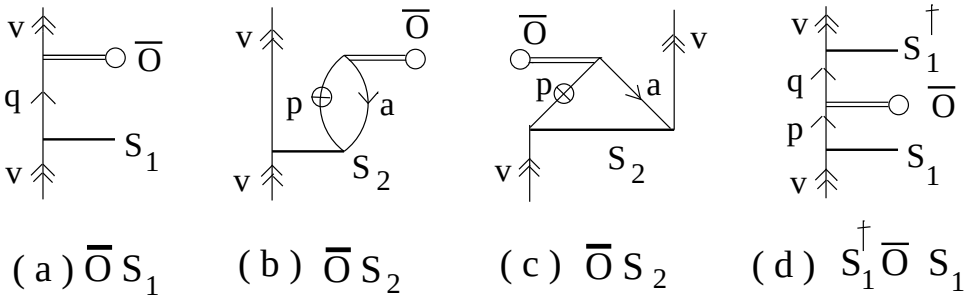

Figure 2: Some many-body diagrams representing the electric quadrupole/hyperfine interaction. Holes (occupied orbitals, labeled by a) and particles are denoted by the lines directed downward and upward respectively. The double line represents the interaction vertex. The valence (labeled by v) and virtual orbitals (labeled by $p, q, r..$) are depicted by double arrow and single arrow respectively whereas the orbitals denoted by $\oplus$ can either be valance or virtual.

$$S = S_1 + S_2 = \sum_{k \neq p} \left\{ a_p^\dagger a_k \right\} s_k^p + \sum_{bpq} \left\{ a_p^\dagger a_q^\dagger a_b a_k \right\} s_{kb}^{pq}, \tag{6}$$

where s_k^p and s_{kb}^{pq} denotes the single and double excitation amplitudes for the valence sectors respectively. In Eqs. (5) and (6) we denote the core (virtual) orbitals by $a, b, c... (p, q, r...)$ respectively and k corresponds to the valence orbital.
The corresponding correlated closed shell state is then

$$|\Psi\rangle = \exp(T) |\Phi\rangle . \tag{7}$$

The exact open shell reference state is achieved by using the techniques of electron attachment. In order to add an electron to the kth virtual orbital of the N electron DF reference state we define

$$\left|\Phi_k^{N+1}\right\rangle \equiv a_k^\dagger |\Phi\rangle \tag{8}$$

with the particle creation operator $a_k^\dagger$. Then by using the excitation operators for both the core and valence electron the $(N+1)$ electron exact state is defined as [20]:

$$\left|\Psi_k^{N+1}\right\rangle = \exp(T) \left\{1 + S\right\} \left|\Phi_k^{N+1}\right\rangle . \tag{9}$$

We write the expectation value of any operator O in a normalized form with respect to the exact state $\left|\Psi^{N+1}\right\rangle$ as

$$\langle O \rangle = \frac{\left\langle \Psi^{N+1} \right| O \left| \Psi^{N+1} \right\rangle}{\left\langle \Psi^{N+1} \right| \Psi^{N+1} \rangle} = \frac{\left\langle \Phi^{N+1} \right| \left\{1 + S^\dagger\right\} \exp(T^\dagger) O \exp(T) \left\{1 + S\right\} \left| \Phi^{N+1} \right\rangle}{\langle \Phi^{N+1} | \left\{1 + S^\dagger\right\} \exp(T^\dagger) \exp(T) \left\{1 + S\right\} | \Phi^{N+1} \rangle}. \tag{10}$$

For computational simplicity we store only the one-body matrix element of $\overline{O} = \exp(T^\dagger) O \exp(T)$. $\overline{O}$ may be expressed in terms of uncontracted single-particle lines [21]. The fully contracted part of $\overline{O}$ will not contribute as it cannot be *linked* with the remaining part of the numerator of the above equation. First few terms of Eq.(10) can be identified as $\overline{O}$, $\overline{O}S_1$ and $\overline{O}S_2$ which we identify as dressed Dirac-Fock (DDF), dressed pair-correlation (DPC) and dressed core-polarization (DCP) respectively. The other terms are being identified as , $S_1^\dagger \overline{O} S_1$, $S_1^\dagger \overline{O} S_2$, $S_2^\dagger \overline{O} S_1$ and $S_2^\dagger \overline{O} S_2$ and are classified as higher order effects. We use the term 'dressed' to describe the modification of the operator O due to core-core correlation effects. In Fig. 2 we replace the operator O by the dressed operator $\overline{O}$ (the dressed quadrupole/hyperfine interaction operator) which includes the core excitation effects and the respective figures are termed as 2(a) $\overline{O}S_1$, 2(b+c) $\overline{O}S_2$ and 2(d) $S_1^\dagger \overline{O} S_1$. Here 2(a) and 2(b+c) represent the DPC and DCP effects respectively. 2(b) is known as the direct and 2(c) is the exchange DPC diagram. Figure 2(d) refers to one of the higher order pair correlation effect which belongs to the set, termed as 'others'.

3 Electric quadrupole shift

The largest source of systematic frequency shift for the clock transition in Sr^+ arises from the electric quadrupole shift of the $4d^2D_{5/2}$ state caused by its electric quadrupole moment of that state and the

interaction of the external electric field gradient present at the position of the ion. The electric quadrupole moment in the state $4d\ ^2D_{5/2}$ was measured experimentally by Barwood *et al.* at NPL [22]. Since the ground state $5s\ ^2S_{1/2}$ does not possess any electric quadrupole moment, the contribution to the quadrupole shift for the clock frequency comes only from the $4d\ ^2D_{5/2}$ state.

The interaction of the atomic quadrupole moment with the external electric-field gradient is analogous to the interaction of a nuclear quadrupole moment with the electric fields generated by the atomic electrons inside the nucleus. In the presence of the electric field, this gives rise to an energy shift by coupling with the gradient of the electric field. Thus the treatment of electric quadrupole moment is analogous to its nuclear counterpart. The quadrupole moment $\mathbf{\Theta}$ of an atomic state $|\Psi(\gamma, J, M)\rangle$ is defined as the diagonal matrix element of the quadrupole operator with the maximum value M_J, given by

$$\mathbf{\Theta} = \langle \Psi(\gamma JJ)| \, \Theta_{zz} \, |\Psi(\gamma JJ)\rangle \ . \tag{11}$$

Here γ is an additional quantum number which distinguishes the initial and final states. The electric quadrupole operator in terms of the electronic coordinates is given by

$$\Theta_{zz} = -\frac{e}{2} \sum_j \left(3z_j^2 - r_j^2\right), \tag{12}$$

where the sum is over all the electrons and z is the coordinate of the jth electron. To calculate the quantity we express the quadrupole operator in its single particle form as

$$\Theta_m^{(2)} = \sum_m q_m^{(2)}. \tag{13}$$

More details about evaluation of electric quadrupole moment using RCC theory is described in our recent paper [23]. The electric quadrupole shift is evaluated using the relation

$$\langle \Psi(\gamma JFM_F)| \, \Theta \, |\Psi(\gamma JFM_F)\rangle = \frac{-2A\left[3M_F^2 - F(F+1)\right] \langle \Psi(\gamma JF) \| \, \Theta^{(2)} \, \| \Psi(\gamma JF)\rangle}{\left[(2F+3)(2F+2)(2F+1)2F(2F-1)\right]^{1/2}} \times \mathcal{O}(\alpha, \beta) \tag{14}$$

and

$$\mathcal{O}(\alpha, \beta) = \left[(3\cos^2\beta - 1) - \epsilon(\cos^2\alpha - \sin^2\alpha)\right]. \tag{15}$$

Here γ specifies the electronic configuration of the atoms and F and M_F are the total atomic angular momentum (nuclear + electronic) and its projection; α and β are the two of the three Euler angles that take the principal-axis frame of the electric field gradient to the quantization axis and ϵ is an asymmetry parameter of the electric potential function [24].

4 Hyperfine shift

The frequency standard is based on the ^{88}Sr isotope. In addition to $^{88}Sr^+$, the odd isotope $^{87}Sr^+$ has also been proposed as a possible candidate for an optical frequency standard [25]. An experiment has been performed in NPL to measure the hyperfine structure of the $4d\ ^2D_{5/2}$ state in $^{87}Sr^+$[25]. Theoretical determination of hyperfine constants is one of most stringent tests of accuracy of the atomic wave functions near the nucleus. Also accurate predictions of hyperfine coupling constants require a precise incorporation of relativistic and correlation effects.

Unlike the even isotope ($^{88}Sr^+$) of strontium ion, $^{87}Sr^+$ has a non zero nuclear spin ($I = \frac{9}{2}$) and the $m_F = 0$ levels for both the $^2S_{1/2}$ and $^2D_{5/2}$ states are independent of the first order Zeeman shift. Here, in table 2 we present the results of our calculation of the magnetic dipole (A) hyperfine constant for the $5s\ ^2S_{1/2}$ and $4d\ ^2D_{5/2}$ states and the electric quadrupole hyperfine constant (B) for the $4d\ ^2D_{5/2}$ state of $^{87}Sr^+$ and compare with the measured values. More details of our calculation can be found in Ref [26].

The hyperfine interaction is given by

$$H_{hfs} = \sum_k M^{(k)} \cdot T^{(k)}, \tag{16}$$

where $M^{(k)}$ and $T^{(k)}$ are spherical tensors of rank k, which corresponds to nuclear and electronic parts of the interaction respectively. The lowest $k = 0$ order represents the interaction of the electron with the spherical part of the nuclear charge distribution.

In the first order perturbation theory, the energy corresponding to the hyperfine interaction of the fine structure state $|JM_J\rangle$ are the expectation values of H_{hfs} such that

$$\begin{aligned} W(J) &= \langle IJFM_F| \sum_k M^{(k)} \cdot T^{(k)} |IJFM_F\rangle \\ &= \sum_k (-1)^{I+J+F} \left\{ \begin{array}{ccc} I & J & F \\ J & I & k \end{array} \right\} \langle I\| M^{(k)} \|I\rangle \langle J\| T^{(k)} \|J\rangle \ . \end{aligned} \tag{17}$$

Here $\mathbf{I}$ and $\mathbf{J}$ are the total angular angular momentum for the nucleus and the electron state, respectively, and $\mathbf{F} = \mathbf{I} + \mathbf{J}$ with the projection M_F.

4.1 Magnetic dipole hyperfine constant

Hyperfine effects arise due to the interaction between the various moments of the nucleus and the electrons of an atom. Nuclear spin gives rise to a nuclear magnetic dipole moment which interacts with the electrons and thus gives rise to magnetic dipole hyperfine interaction defined by the magnetic dipole hyperfine constant A. For an eigen state $|IJ\rangle$ of the Dirac-Coulomb Hamiltonian, A is defined as

$$A = \mu_N \left(\frac{\mu_I}{I}\right) \frac{\langle J\| T^{(1)} \|J\rangle}{\sqrt{J(J+1)(2J+1)}}, \tag{18}$$

where μ_I is the nuclear dipole moment defined in units of Bohr magneton μ_N. The magnetic dipole hyperfine operator $T^{(1)}_q$ which is a tensor of rank 1 can be expressed in terms of single particle rank 1 tensor operators and is given by the first order term of Eq. (17)

$$T^{(1)}_q = \sum_q t^{(1)}_q = \sum_j -ie\sqrt{\frac{8\pi}{3}} r_j^{-2} \overrightarrow{\alpha_j} \cdot \mathbf{Y}^{(0)}_{1q}(\widehat{r_j}) \, . \tag{19}$$

Here $\overrightarrow{\alpha}$ is the Dirac matrix and $\mathbf{Y}^{\lambda}_{kq}$ is the vector spherical harmonics. The index j refers to the j-th electron of the atom with r_j its radial distance and e is the magnitude of the electronic charge.

4.2 Electric quadrupole hyperfine constant

The second order term in the hyperfine interaction is the electric quadrupole part. The electric quadrupole hyperfine constant is defined by putting $k = 2$ in Eq. (17). The nuclear quadrupole moment is defined as

$$T^{(2)}_q = \sum_q t^{(2)}_q = \sum_j -er_j^{-3} C^{(2)}_q(\widehat{r_j}), \tag{20}$$

Here, $C^{(k)}_q = \sqrt{\frac{4\pi}{(2k+1)}} Y_{kq}$, with Y_{kq} being the spherical harmonic. Hence the electric quadrupole hyperfine constant B in terms of the nuclear quadrupole moment Q_N is

$$B = 2eQ_N \left[\frac{2J(2J-1)}{(2J+1)(2J+2)(2J+3)}\right]^{1/2} \langle J\| T^{(2)} \|J\rangle \, . \tag{21}$$

The corresponding shift in the energy levels are known an hyperfine shift which is expressed as

$$W_{hyp} = W_{M1} + W_{E2} = A\frac{K}{2} + \frac{B}{2}\frac{3K(K+1) - 4I(I+1)J(J+1)}{2I(2I-1)2J(2J-1)}, \tag{22}$$

where $K = F(F+1) - I(I+1) - J(J+1)$.

Table 1: Electric quadrupole moment for the $4d\ ^2D_{5/2}$ state of $^{88}Sr^+$ in units of ea_0^2. PW corresponds to our present CCSD(T) calculation and MCDF for Multi-configuration Dirac-Fock.

	PW	MCDF [27]	Experiment [22]
$4d_{5/2}$	2.94	3.02	2.6±0.3

5 Results and discussions

The occupied and the virtual orbitals used in the calculation are obtained by solving the Dirac-Fock (DF) equation for Sr^{++} for a finite Fermi nuclear distribution. These orbitals are linear combinations of Gaussian type functions on a grid [28]. The open shell coupled cluster (OSCC) method is used to construct different single valence states whose reference states correspond to adding a particle to the closed shell reference state. We use the singles-doubles and partial triples approximation, abbreviated as CCSD(T) and excitations from all the core orbitals have been considered. We have estimated the error incurred in our present work, by taking the difference between our RCC calculations with singles, doubles as well as the most important triple excitations (CCSD(T)) and only single and double excitations (CCSD).

5.1 Electric quadrupole moment

We present our results of the electric quadrupole moment for the $4d\ ^2D_{5/2}$ state of $^{88}Sr^+$ in table 1. The value of $\mathbf{\Theta}$ in the $4d\ ^2D_{5/2}$ state measured experimentally is $(2.6 \pm 0.3)ea_0^2$ [22]. Our calculated value for the $4d\ ^2D_{5/2}$ stretched state is $(2.94 \pm 0.07)ea_0^2$, where e is the electronic charge and a_0 is the Bohr radius. We analysed our results and have found that the DDF contribution is the largest. The leading contribution to electron correlation comes from the DPC effects and the DCP effects are an order of magnitude smaller. This can be understood from the DPC diagram (Fig.2(a)) which has a valence electron in the $4d_{5/2}$ state. Hence the dominant contribution to the electric quadrupole moment arises from the overlap between virtual $d_{5/2}$ orbitals and the valence, owing to the fact that S_1 is an operator of rank 0 and the electric quadrupole matrix elements for the valence $4d_{5/2}$ and the diffuse virtual $d_{5/2}$ orbitals are substantial. On the other hand, in the DCP diagram (Fig.2(b+c)), the matrix element of the same operator could also involve the less diffuse s or p orbitals. Hence, for a property like the electric quadrupole moment, whose magnitude depends on the square of the radial distance from the nucleus, this trend seems reasonable, whereas for properties like hyperfine interaction which is sensitive to the near nuclear region, the trend is just the opposite for the d states [29]. As expected, the contribution of the DHOPC effect i.e., $S_1^\dagger \bar{O} S_1$ (Fig.2(d)) is relatively important as it involves an electric quadrupole matrix element between the valence $4d_{5/2}$ and a virtual $d_{5/2}$ orbital.

5.2 Hyperfine constants

The magnetic dipole (A) and electric quadrupole (B) hyperfine constants for the of $^{87}Sr^+$ are given in table 2 along with the calculated and experimental results. The $g_i = \mu_N \left(\frac{\mu_I}{I}\right)$ value used for the calculation is from Ref. [30]. PW corresponds to the 'present work' using CCSD(T). CC stands for coupled-cluster calculation by Martensson-Pendrill [31] and Nayak and Chaudhuri [32], DF-AO for Dirac-Fock with all order core polarization effect by Yu *et al.* and the column 'others' refers to the calculation by Yuan *et al.* using relativistic linked cluster many-body perturbation theory (RLCMBPT) [33] and by one of the authors using relativistic effective valence shell Hamiltonian method [34]. Information on A for the $4d\ ^2D_{5/2}$ state is very important in connection with optical frequency standards [12, 25]. The measured value of this quantity is 2.1743 ± 0.0014 MHz [25], whereas the previously calculated values vary from 1.07 MHz [31] and 2.507 MHz [35]. Our calculated value of A is 2.16 ± 0.02 MHz; this is the most accurate theoretical determination of A for the $4d\ ^2D_{5/2}$ state to date. For the $5s\ ^2S_{1/2}$state our calculated value of A is 997.26 ± 0.03 MHz. To analyze the result we focus on the various many-body effects contributing to the calculation of A. The most important many-body diagrams are presented in Fig. 2. We have noticed that for $5s\ ^2S_{1/2}$ state the dominant contribution is at the DDF level $\sim 72\%$. However, for the $4d\ ^2D_{5/2}$ state the DCP effect is larger and its sign is opposite that of the DDF contribution. In their calculations Martensson [31] and Yu *et al.* [35] have found similar trends. We have seen that the higher order correlation effects contribute significantly in determining A for this

Table 2: Magnetic dipole (A) hyperfine constant for the $5s\,^2S_{1/2}$ and $4d\,^2D_{5/2}$ states and the electric quadrupole hyperfine constant (B) for $4d\,^2D_{5/2}$ state of $^{87}Sr^+$ in MHz.

		PW	CC	DF-AO [35]	Others	Experiment
$5s_{1/2}$	A	-997.26	-1000 [31]	-1003.18	-987 [33]	-1000.5±1.0 [36]
			-999.89 [32]		-1005.74 [34]	-990 [37]
						-993.5 [38]
						-1000.473 673 [39]
$4d_{5/2}$	A	2.16	1.07 [31]	2.51		2.1743±0.0014 [25]
			1.87 [32]			
	B	47.8	54.4 [31]			49.11±0.06 [36]
			51.12 [32]			

state - collectively they are 60% of the total value but opposite in sign. In the earlier calculations the determination of the higher order effects was not as accurate as ours.

The calculated value for the electric quadrupole hyperfine constant (B) for the $4d\,^2D_{5/2}$ state is 47.8 ± 0.2 MHz which deviates $\sim 2.7\%$ from the central experimental value. The earlier determination of B was off by $\sim 11\%$ from the experiment. Since the other state involved in the clock transition is spherically symmetric the electric quadrupole hyperfine constant is zero and there will be no hyperfine shift due to B for the $5s\,^2S_{1/2}$state.

From the figure presented in Fig. 2 it is clear that the DPC effect involves the hyperfine interaction of a valence electron and the residual Coulomb interaction, i.e for $5s\,^2S_{1/2}$ state the hyperfine matrix element becomes $\langle [4p^6]5s_{1/2}\,|h_{hfs}|\,[4p^6]q\rangle$, where q can be any virtual orbital and h_{hfs} is the single-particle hyperfine operator. Since only $s_{1/2}$ and $p_{1/2}$ electrons have a sizable density in the nuclear region, the DPC effect is dominant for $5s_{1/2}$ state but not for the $4d_{5/2}$ state. On the other hand, the DCP effects represent the hyperfine interaction of a polarized core electron with any virtual electron (see Fig. 2b,c). For $4d_{5/2}$ state it is clear that the hyperfine matrix element for the DPC effect is much smaller than the DCP effect, which plays the most important role in determining the value of A. The core polarization contribution is so large for this state that it even dominates over the DDF contribution.

6 Conclusion

In conclusion, we have performed an *ab initio* calculation of the electric quadrupole moment for the $4d\,^2D_{5/2}$ state of $^{88}Sr^+$ to an accuracy of less than 2.5% using the RCC theory. This is the first application of RCC theory to determine the electric quadrupole moment (EQM) of any atom and is currently the most accurate determination of EQM for the $4d\,^2D_{5/2}$ state in Sr^+. We have also calculated the magnetic dipole (A) hyperfine constant for the $5s\,^2S_{1/2}$ and $4d\,^2D_{5/2}$ states and electric quadrupole hyperfine constant (B) for the $4d\,^2D_{5/2}$ state of $^{87}Sr^+$. Evaluation of correlation effects to all orders as well as the inclusion of the dominant triple excitations in our calculation was crucial in achieving this accuracy. The magnitude of electric quadrupole moment depends on the square of the radial distance from the nucleus, whereas properties like hyperfine interaction are sensitive to the near nuclear region. The accurate determination of quantities like electric quadrupole moment and hyperfine constants establish the fact that RCC is very powerful and efficient method for determining atomic properties near the nuclear region as well as at large distances from the nucleus. Our result will lead to a better quantitative understanding of the electric quadrupole shift of the resonance frequency of the clock transition in Sr^+.

Acknowledgments : Financial support from the BRNS, DAE for project no. 2002/37/12/BRNS is gratefully acknowledged. The computations are carried out in our group's Xeon and the Opteron computing cluster at IIA.

References

[1] J.C. Bergquist, S. R. Jefferts, and D. J. Wineland, *Physics Today*, **54**, No.3, 37, (2001).

[2] W. M. Itano, Proc. *IEEE*, **79**, 936-942 (1991).

[3] W. M. Itano and N.F. Ramsey, *Sci. Am.*, **269**, 56-65 (1993).

[4] `http://tf.nist.gov/cesium/atomichistory.htm`

[5] L. Hollberg *et al.*, *J. Phys. B*, **38**, S469-S495 (2005).

[6] J. E. Bernard *et al.*, *Phys. Rev. Lett.,* **82**, 3228 (1999).

[7] H. S. Margolis *et al.*, *Phys. Rev. A*, **67**, 032501 (2003).

[8] R. Rafac *et al., Phys. Rev. Lett.*, **85**, 2462 (2000).

[9] J. Stenger *et al.*, *Opt. Lett.*, **26**, 1589 (2001).

[10] C. Champenois *et al.*, *Phys. Lett. A*, **331**, 298 (2004).

[11] P. Gill and H. Margolis, *Physics World*, 35, May (2005).

[12] H. S. Margolis *et al.*, *Science*, **306**, 1355 (2004).

[13] W. H. Oskay, W. M. Itano and J. C. Bergquist, *Phys. Rev. Lett.,* **94**, 163001 (2005).

[14] W. M. Itano, NIST, *Private Communications.*

[15] I. P Grant, *Phys. Scr.,* **21**, 443 (1980).

[16] S. A. Blundell, W. R. Johnson and J. Sapirstein, *Phys. Rev. A*, **43**, 3407 (1991).

[17] D. Mukherjee and S. Pal, *Adv. Quant. Chem.*, **20**, 281 (1989) and the references therein.

[18] U. Kaldor, *Lecture Notes in Physics, Microscopic Quantum many-body theories and their applications,* p.71, Eds. J. Navarro and A. Polls, Springer-Verlag-Berlin, Heidelberg and New York (1998) and references therein.

[19] B. P. Das *et al.*, *J. Theor. and Comp. Chem.*, **4**, 1 (2005) and references therein.

[20] I. Lindgren and J. Morrison, *Atomic Many-Body Theory* (Springer, Berlin) 1985.

[21] G. Gopakumar *et al.*, *Phys. Rev. A.*, **64**, 032502 (2001).

[22] G. P. Barwood *et al.*, *Phys. Rev. Lett.* **93**, 133001 (2004).

[23] C. Sur *et al.*, *Phys. Rev. Lett.* **96**, 193001 (2006).

[24] P. Dube *et al.*, *Phys. Rev. Lett.* **95**, 033001 (2005).

[25] G. P. Barwood, K. Gao, P. Gill, G. Huang and H. A. Klein, *Phys. Rev. A*, **67**, 013402 (2003).

[26] C. Sur *et al.*, (Submitted to *J. Phys. B* 2006).

[27] W. Itano, *Phys. Rev. A*, **73**, 022510 (2006).

[28] R. K. Chaudhuri, P. K. Panda and B. P. Das, *Phys. Rev. A*, **59**, 1187 (1999).

[29] C. Sur, B. K. Sahoo, R. K. Chaudhuri, B. P. Das and D. Mukherjee, *Eur. Phys. J. D*, **32**, 25 (2005).

[30] `http://www.webelements.com`

[31] A. M. Martensson-Pendrill, *J. Phys. B*, **35**, 917 (2002).

[32] M. K. Nayak and R. K. Chaudhuri, *Eur. Phys. J. D*, **37**, 171 (2006).

[33] X Yuan *et al.*, *Phys. Rev. A.*, **52**, 197 (1995).

[34] R. K. Chaudhuri, K. Freed, *J. Chem Phys.*, **122**, 204111 (2005).

[35] K. Yu, L. Wu, B. Gou and T. Shi, *Phys. Rev. A*, **70**, 012506 (2004).

[36] F. Buchinger *et al.*, *Phys. Rev. A*, **41**, 2883 (1990).

[37] R. Beignang, W. Makat, A. Timmermann and P. J. West, *Phys. Rev. Lett.*, **51**, 771 (1983).

[38] K. T. Lu, J-Q Sun and R. Beignang, *Phys. Rev. A*, **37**, 2220 (1988).

[39] H. Sunaoshi *et al.*, *Hyperfine Interact.*, **78**, 241(1993).